Photoacoustics 34 (2023) 100571

Contents lists available at ScienceDirect

Photoacoustics

journal homepage: www.elsevier.com/locate/pacs

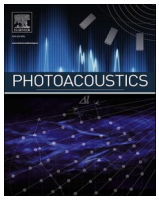

All-optical non-resonant photoacoustic spectroscopy for multicomponent gas detection based on aseismic photoacoustic cell

Lujun Fu [a,b], Ping Lu [a,b,c,*], Yufeng Pan [a], Yi Zhong [a], Chaotan Sima [a,b,c], Qiang Wu [d], Jiangshan Zhang [e], Lingzhi Cui [f,**], Deming Liu [a,b]

[a] Wuhan National Laboratory for Optoelectronics (WNLO) and National Engineering Research Center for Next Generation Internet Access System, School of Optical and Electronic Information, Huazhong University of Science and Technology, Wuhan 430074, China
[b] Shenzhen Huazhong University of Science and Technology Research Institute, Shenzhen 518000, China
[c] Wuhan OV Optical Networking Technology Co., Ltd., Wuhan 430073, China
[d] Faculty of Engineering and Environment, Northumbria University, Newcastle Upon Tyne NE1 8ST, United Kingdom
[e] Department of Electronics and Information Engineering, Huazhong University of Science and Technology, Wuhan 430074, China
[f] State Key Laboratory of NBC Protection for Civilian, Beijing 102205, China

ARTICLE INFO

Keywords:
Optical microphone
Photoacoustic spectroscopy
Multicomponent gas detection
Silicon cantilever
Aseismic photoacoustic cell

ABSTRACT

An all-optical non-resonant photoacoustic spectroscopy system for multicomponent gas detection based on a silicon cantilever optical microphone (SCOM) and an aseismic photoacoustic cell is proposed and demonstrated. The SCOM has a high sensitivity of over 96.25 rad/Pa with sensitivity fluctuation less than ± 1.56 dB between 5 Hz and 250 Hz. Besides, the minimal detectable pressure (MDP) of the sensor is 0.55 μPa·Hz$^{-1/2}$ at 200 Hz, which indicates that the fabricated sensor has high sensitivity and low noise level. Six different gases of CO_2, CO, CH_4, C_2H_6, C_2H_4, C_2H_2 are detected at the frequency of 10 Hz, whose detection limits (3σ) are 62.66 ppb, 929.11 ppb, 1494.97 ppb, 212.94 ppb, 1153.36 ppb and 417.61 ppb, respectively. The system achieves high sensitivity and low detection limits for trace gas detection. In addition, the system exhibits seismic performance with suppressing vibration noise by 4.5 times, and achieves long-term stable operation. The proposed non-resonant all-optical PAS multi-component gas detection system exhibits the advantages of anti-vibration performance, low gas consumption and long term stability, which provides a solution for working in complex environments with inherently safe.

1. Introduction

In consideration of the complexity of the application environment where many components are existed, the actual process requires multi-component gas detection, and the content of each component gas needs to be monitored [1,2]. For example, the online detection of the dissolved gases concentration in oil of transformer is always an important characteristic to discriminate the transformer operation status [3,4]. Therefore, the technology of simultaneous detection of multi-component gas is particularly important. Tunable diode laser absorption spectroscopy (TDLAS) [5,6] and photoacoustic spectroscopy (PAS) [7–10] has been widely studied due to their specific selectivity, high sensitivity and fast response, by using absorption spectroscopy to detect trace gases. For TDLAS technology, photodetector (PD) is required. It is necessary to use high-power lasers to achieve lower gas detection limits for TDLAS. And to detect different gases, lasers of different wavelength are required. So higher requirements are put forward for PDs in TDLAS. However, only the magnitude of sound pressure needs to be detected in PAS. Therefore, PAS has unique advantages in multi gas detection.

PAS is an important technology to realize trace gas detection based on photoacoustic effect. It has the advantages of high sensitivity, high selectivity, large dynamic detection range and real-time online monitoring. It plays an important role in trace gas detection. Various kinds of photoacoustic spectral gas detection structures have been reported such as T-type cell [11,12], H-type resonant PAS [13–15], two channel

* Corresponding author at: Wuhan National Laboratory for Optoelectronics (WNLO) and National Engineering Research Center for Next Generation Internet Access System, School of Optical and Electronic Information, Huazhong University of Science and Technology, Wuhan 430074, China.
** Corresponding author.
E-mail addresses: pluriver@mail.hust.edu.cn (P. Lu), cuilz@pku.edu.cn (L. Cui).

https://doi.org/10.1016/j.pacs.2023.100571
Received 23 August 2023; Received in revised form 10 October 2023; Accepted 6 November 2023
Available online 9 November 2023
2213-5979/© 2023 The Author(s). Published by Elsevier GmbH. This is an open access article under the CC BY-NC-ND license (http://creativecommons.org/licenses/by-nc-nd/4.0/).

differential resonant PAS [16–18] and the quartz-enhanced photoacoustic spectroscopy (QEPAS) [19,20]. The resonant structure has higher detection sensitivity via resonant amplifying. However, the photoacoustic signal could be unstable while the resonant frequency drift in complex application environments. As for QEPAS, the long-term instability also exist while working at the resonant frequency of 32.7 kHz [20,21]. Although beat frequency QEPAS can effectively suppress the impact of sensitivity drift near the resonant frequency, the experimental system is complicated [22]. And laser sources are usually used in these structures. However, due to the narrow tunable range of the near-infrared tunable laser and the coincidence of the gas in near-infrared spectrum, a single near-infrared tunable laser is rarely used in the detection of multi-component gases [23]. Besides, a sensitive multi-gas analyzer based on multiple lasers is complicated and costly. Though high sensitive microphone is beneficial for improving system response because of their high sensitivity to detect acoustic pressure, it's also sensitive to external vibration in PAS gas detection, which brings difficulties to applied in the actual complex environment with high stability [8]. Therefore, the seismic resistant PAS system for multicomponent gas detection is urgently demanded.

In this work, a non-resonant PAS based on a silicon cantilever optical microphone (SCOM) and an aseismic PAC structure is proposed and demonstrated for multicomponent gas detection. A Fabry-Perot interference (FPI)-based low-frequency SCOM based on the Micro-Electromechanical systems (MEMS) technology is designed and fabricated. Experiments show that the fabricated SCOM has a strong response at low frequency, which exhibit higher sensitivity than traditional diaphragm sensors [24–26]. The pressure responsivity is measured to be over 96.25 rad/Pa with sensitivity fluctuation less than ± 1.56 dB between 5 Hz and 250 Hz. And the minimal detectable pressure (MDP) of the sensor is 0.55 μPa·Hz$^{1/2}$ at 200 Hz. The noise performance of the SCOM is far superior to that of commercial condenser microphones [27,28]. The structure of PAC is theoretical designed to immune to external vibration. The vibration insensitive of the PAS is greatly improved by 4.5 times through the mechanical methods, while ensuring the miniaturization with the gas consumption of only 2.15 mL. Six different gases of CO_2, CO, CH_4, C_2H_6, C_2H_4, C_2H_2 are detected at the designed PAS system, with the detection limits (3σ) of 62.66 ppb, 929.11 ppb, 1494.97 ppb, 212.94 ppb, 1153.36 ppb and 417.61 ppb, respectively. And the experimental results verify the system has long-term stability. The proposed non-resonant all-optical PAS multi-component gas detection system exhibits the advantages of anti-vibration performance, low gas consumption and long term stability, which provides a solution for working in complex environments with inherently safe.

2. Theoretical analysis and structure design

The signal to noise ratio (SNR) of the system determines the performance of the PAS to a large extent, and it is related to the performance of the microphone and the structure of the photoacoustic cell. The microphone based on silicon cantilever has an excellent response to the acoustic wave, so that the response can be easily affected by the external vibration disturbances due to its high sensitivity. However, the minimum detection limit of the PAS system is determined by SNR, which is affected by the external environmental noise. And SCOM is usually sensitive to external vibration but not to external sound signal since it's usually placed in an enclosed metal cell in PAS gas detection, which brings difficulties to applied in the actual complex environment with high stability. Meanwhile the structure of the photoacoustic cell determines the intensity of the acoustic signal produced by photoacoustic effect. In order to address these issues, a vibration-insensitive photoacoustic cell structure with two chambers is proposed. One chamber is used as photoacoustic cell to generate acoustic wave, while the other is placed nearby connected with the SCOM by a micro pinhole, in which the center of gravity of the microphone's rear cavity is changed. Compared with single chamber structure, the opposite force will be exerted on the cantilever beam in the vibration environment to resist acceleration noise.

For common photoacoustic cells, the microphone is placed in the middle of the photoacoustic cell where the top of the microphone is flush with the inner wall of the cell, as shown in Fig. 1(a). When the photoacoustic cell is around with vibration noise, for example acceleration vibration to the right, the equivalent inertial force direction of the cantilever beam itself F_1 is the same with the inertial force direction of the air besides the cantilever F_2 which points to the left, as shown in Fig. 1(b). It's similar while the acceleration vibration turns to the left, where the equivalent pressures are all to the right. In this case, the photoacoustic cell inevitably introduces additional vibration noise, which is difficult to eliminate when the vibration frequency coincides with the working frequency. Though these acceleration vibration noise can be suppressed or even eliminated using the double microphone system [8], there is also another method to decrease these kinds of disturbances with a single cantilever beam microphone which greatly simplifies the photoacoustic spectroscopy system. In order to reduce the impact of external acceleration vibration noise, a vibration-resistant photoacoustic cell structure with only one microphone is designed, in which the center of gravity of the back cavity is offset, as shown in Fig. 1(c). When the photoacoustic cell is placed in the vibration noise environment, for example acceleration vibration noise to the right, the equivalent inertial force direction of the cantilever beam itself F_1 is contrary with the inertial force direction of the air besides the cantilever F_2. When designing the structure of the photoacoustic cell reasonably, it is possible for two opposing forces to completely cancel each other out, as shown in Fig. 1(d). The combined force caused by the cantilever beam and air inertia on the cantilever can be described as [29]:

$$p_{\text{eff}} = a(\rho_{\text{can}} d + \rho_{\text{air}} D) \tag{1}$$

where a is the magnitude of acceleration noise, ρ_{can} is the density of cantilever, d is the thickness of cantilever, ρ_{air} is the density of air in the PAC, D is the distance of the center of PAC and chamber located behind the cantilever beam. When the center of chamber is further away from cantilever compared with PAC, the value of D should be negative. In order to achieve aseismic effect, it is necessary to make the effective sound pressure p_{eff} to be zero. At this point, the spacing D should satisfy the following expression:

$$D = -\frac{\rho_{\text{can}}}{\rho_{\text{air}}} d \tag{2}$$

Because the density of cantilever and gases, and the thickness of the cantilever is already known, the spacing D can be accurately calculated by Eq. (2). According to the aseismic theory analyzed in the previous stage, a proper geometrical design of PAC has been proposed and processed to compensate the vibration noise.

3. Experimental results and discussions

3.1. Experimental tests of optical microphone

An optical microphone based on silicon cantilever structure by using MEMS technology is used to detect the photoacoustic pressure. The integrated SCOM includes a silicon cantilever coated with gold, a stainless steel shell, a ceramic ferrule and an optical fiber, which builts Fabry-Perot (FP) interference cavity, as shown in Fig. 2(a). The reflection spectrum of the produced SCOM is shown in Fig. 2(b). The schematic diagram of testing equipment for obtaining reflection spectra can refer to Fig. 3(b) of Ref [26]. The free spectral range (FSR) is 3.3 nm according to the interference spectrum and the FP cavity length of the SCOM is calculated to be 360 μm. The length of FP cavity changes while photoacoustic signal is generated. The reflection spectrum of the produced SCOM shifts left and right when acoustic pressure is applied to the silicon cantilever beam. In order to accurately evaluate the performance of

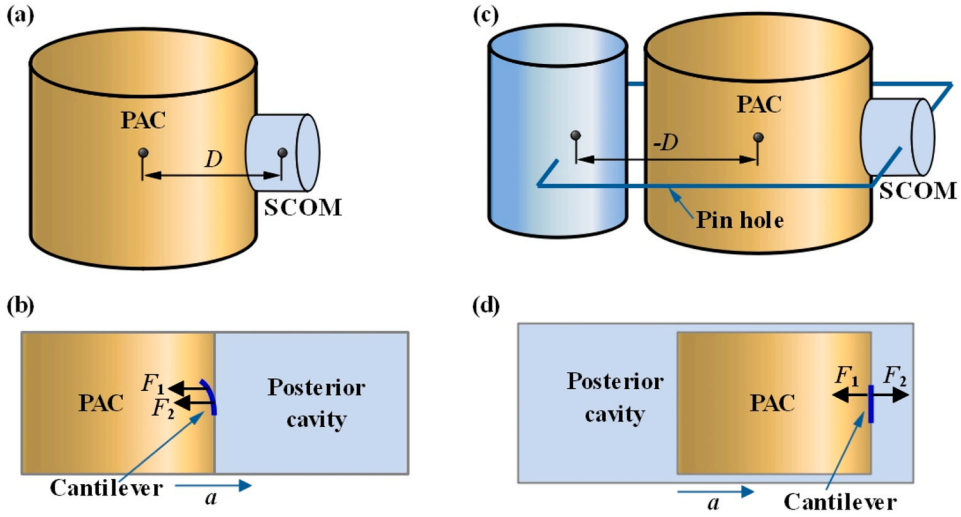

Fig. 1. Schematic diagram of (a) a conventional structure and (b) its response to vibration acceleration conditions, (c) an aseismic structure and (d) its response to vibration acceleration conditions.

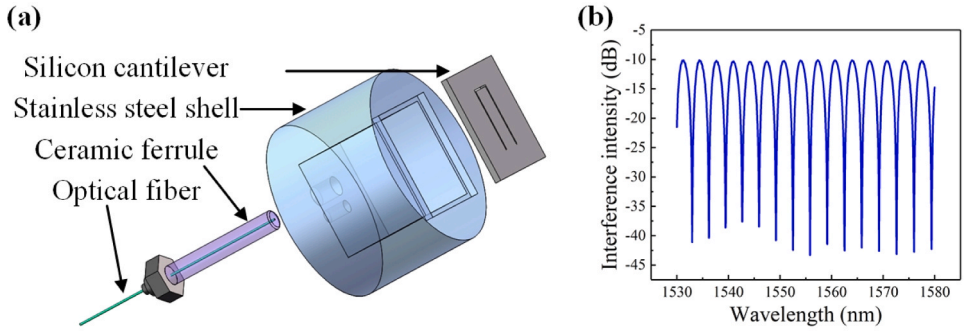

Fig. 2. (a) Schematic diagram of the installed SCOM. (b) The reflection spectrum of the produced SCOM.

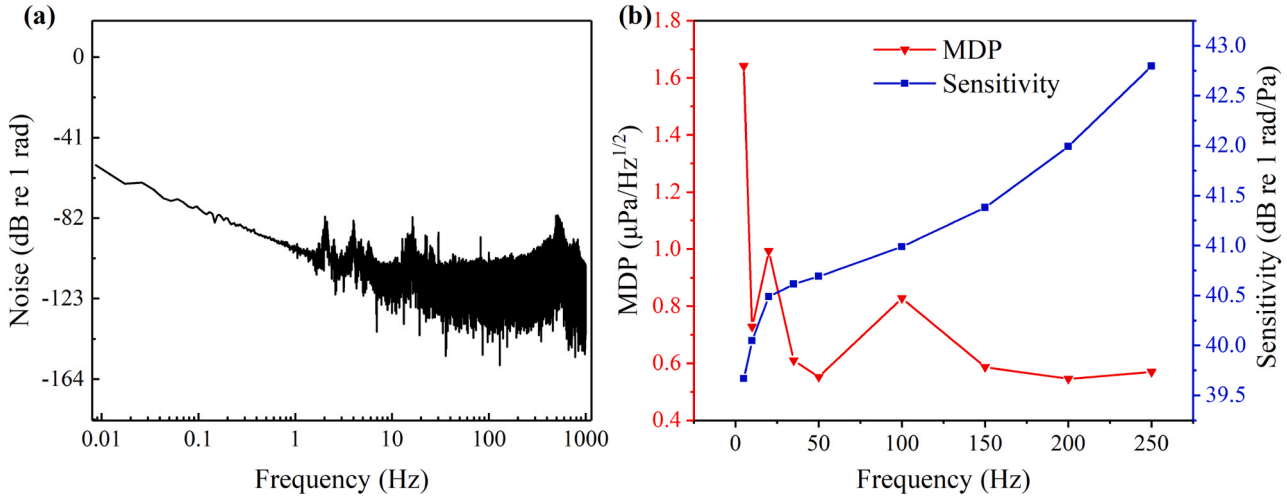

Fig. 3. (a) Noise characteristics of fabricated SCOM at anechoic chamber. (b) Acoustic sensitivity and minimal detectable pressure (MDP) for the frequency range of 5–250 Hz.

the produced SCOM sensor, an acoustic experimental setup is built. For details, please refer to the section 1.2 of reference [8].

To obtain the response of the fabricated sensor, sinusoidal sound waves are applied with the frequency from 5 Hz to 250 Hz. A sinusoidal fitting is used to achieve the amplitude of demodulated phase signal, in which the results are more precise compared with the common methods such as subtraction with maximum and minimum data point or extracting peak value after fast Fourier Transform (FFT) [26]. In order to obtain the performance parameters of microphone, the noises of SCOM are detected in an anechoic chamber. The noises, frequency response

and MDP are demonstrated in Fig. 3. The noise spectrum after FFT at anechoic chamber is shown in Fig. 3(a). The experimental data of the measured frequency response and MDP from 5 Hz to 250 Hz is demonstrated in Fig. 3(b). The experimental results indicate that the fabricated SCOM has ultra-high sound pressure sensitivity, which is above 39.67 dB re 1 rad/Pa (96.25 rad/Pa) in the range of 5 Hz and 250 Hz while the sensitivity fluctuation is less than ± 1.56 dB. The transformation relationship between the phase variation and the displacement is $\Delta\varphi = 4\pi/\lambda \cdot n\Delta d$, where λ is the wavelength which is 1.55 μm, n is the refractivity which is 1 with air, $\Delta\varphi$ is the variation of phase, Δd is the variation of the cavity length [30]. The MDP at 200 Hz is calculated to be about 0.55 μPa·Hz$^{-1/2}$. Table 1 lists the comparisons between our work and other reported optical acoustic sensors. It can be observed that the fabricated acoustic sensor has a relatively higher sensitivity and lower noise level, which shows that the noise level of the SCOM is far superior to that of commercial condenser microphones [27, 28].

3.2. PAS system design

A non-resonant all-optical cantilever enhanced PAS system is designed and fabricated by using an aseismic PAC to suppress vibration noise, as shown in Fig. 4. The system consists an infrared (IR) source with an elliptic reflector, a chopper, a turntable with different filters, a cylindrical non-resonant PAC, a SCOM, a control system and phase demodulation devices. The size of cylindrical cell is optimized with the lengths of 19 mm and diameters of 12 mm, respectively. The light source is a 30 W black-body radiation infrared light source. The intensity-modulated light is transmitted to the PAC through the filter with frequency of 10 Hz. In order to accurately obtain the photoacoustic signal in the PAC, phase demodulation and lock-in amplifier is used. The phase demodulation algorithm based on fast Fourier transform can refer to the previous work [32]. The wavelength of infrared thermal radiation broadband light source covers 3 μm ~ 12 μm. When paired with different types of filters, different gases can be detected. To measure CO, CO_2, CH_4, C_2H_6, C_2H_4, C_2H_2, the parameters of the optical filters should be optimized. To avoid the influence of gases other than the gas to be tested, narrowband filters need to be used, and the selection of filters should follow the following principles. First, as the amplitude of the photoacoustic signal is directly proportional to the absorption coefficient of the gas absorption spectral line, it is advisable to choose the spectral line position with a high absorption coefficient, and the transmittance should be as high as possible. Second, in actual measurement, there may be multiple gases, so it is necessary to avoid strong absorption peaks of other gases as much as possible to reduce cross talk when selecting the filter for the gas to be tested. Finally, due to the fact that the gases to be tested usually contains water vapor, the position of the strong absorption peak of water vapor should be avoided within the passband range of the filters. Considering the above three criteria, the specific parameters of the mid-infrared passband filters are selected as listed in Table 2. According to the HITRAN database [33], the absorption coefficient of the six gases and H_2O are shown in Fig. 5, in which the concentration of H_2O is 100 ppm and the concentration of other gases is 1 ppm. The selected filters are annotated with arrows.

Table 1
Comparison of performance indicators.

Material and structure	Sensitivity	MDP	Frequency	Ref.
Phenylene sulfide membrane	0.7 rad/Pa @ 100 Hz	24.1 μPa•Hz$^{-1/2}$ @ 100 Hz	2–250 Hz	[24]
Phenylene sulfide membrane	72.99 nm/Pa @ 20 Hz	0.65 mPa•Hz$^{-1/2}$ @ 20 Hz	20–250 Hz	[25]
Gold membrane	0.3 rad/Pa @ 100 Hz	10.2 mPa•Hz$^{-1/2}$ @ 5 Hz	0.8–250 Hz	[26]
Stainless cantilever	364 nm/Pa @ 1 kHz	8.5 μPa•Hz$^{-1/2}$ @ 1 kHz	50 Hz - 3 kHz	[31]
Silicon cantilever	211.2 nm/Pa @ 1 kHz	5 μPa•Hz$^{-1/2}$ @ 1 kHz	50 Hz - 2 kHz	[30]
Silicon cantilever	112.04 rad/Pa (13.8 μm/Pa) @ 100 Hz	0.55 μPa•Hz$^{-1/2}$ @ 200 Hz	5–250 Hz	[This paper]

3.3. Experimental results

To obtain the responsiveness of each gas, single component gases of different concentrations are injected into the photoacoustic cell with mass flow controller for controlling the gas flow rate of standard gases and pure N_2 gas. Six different gases of CO_2, CO, CH_4, C_2H_6, C_2H_4 and C_2H_2 are detected in turn with the infrared thermal radiation light source at the modulation frequency of 10 Hz. The photoacoustic spectroscopy system is kept at atmospheric pressure and room temperature. Firstly, the PA cell is filled with the detected gases for about one minute to replace the gas inside. Then the system is idle for half a minute, with the chopper and blackbody thermal radiation light source turned on to achieve stable optical power. Afterwards, data collection is conduct, which takes approximately 20 s. Finally, the signal is calculated and solved with the computer. Finally, the system is in standby mode and the next cycle will take 2 min. The entire detection system takes 4 min to obtain a signal for a certain concentration of gas to be tested within each cycle.

Fig. 6 shows the response of the gases with different concentrations. And a linear fit to the data yields straight line with slope of 7.791 mrad/ppm, 0.5423 mrad/ppm, 0.3173 mrad/ppm, 1.197 mrad/ppm, 0.2663 mrad/ppm, 0.5911 mrad/ppm for six different gases of CO_2, CO, CH_4, C_2H_6, C_2H_4 and C_2H_2, respectively. To verify the liner response of the all-optical photoacoustic spectroscopy system for multi-component gas detection, the linear correlation coefficients are obtained. The linear correlation coefficients (R-square value) are calculated to be 0.9978, 0.9989, 0.9949, 0.9887, 0.999, 0.9996 corresponding to CO_2, CO, CH_4, C_2H_6, C_2H_4 and C_2H_2 respectively, which ensures that the response of the PAS system to gas concentration is approximately linear. The standard derivations of the background noises with 21 consecutive test data are analyzed when the PAC is completely filled with pure N_2, which are 0.163 mrad, 0.168 mrad, 0.158 mrad, 0.085 mrad, 0.102 mrad and 0.0823 mrad, as shown in Fig. 7. Accordingly, detection limits (3σ) of CO_2, CO, CH_4, C_2H_6, C_2H_4 and C_2H_2 are calculated to be 62.66 ppb, 929.11 ppb, 1494.97 ppb, 212.94 ppb, 1153.36 ppb and 417.61 ppb, respectively. Experimental results for six different gases are shown in Table 3.

For comparison, performance indicators of carbon dioxide sensors based on absorption spectroscopy are summarized in Table 4. To the best of our knowledge, the detection limit in this work are optimum among previously reported optical PAS carbon dioxide sensors so far. In order to verify the practical stability of the all optical PAS system based on aseismic structure, comparative experiment based on two structures are conducted. The test results of the aseismic structure and the normal structure with the pin hole blocked for detection of pure N_2 using CO_2 filter are shown in Fig. 8, which last 85 min for each test. The standard deviation of normal structures is 0.731 mrad, while the standard deviation of aseismic structure is 0.163 mrad. The standard deviation of the normal structure is about 4.5 times of aseismic structure, which reflects that the designed structure has the effect of resisting vibration. In order to confirm the stability of the produced PAS system, the test for pure N_2 with CO_2 filter is demonstrated as shown in Fig. 9. The test results show that the signal changes by less than 0.6% within 8 h, which indicate the system has a long-term stability.

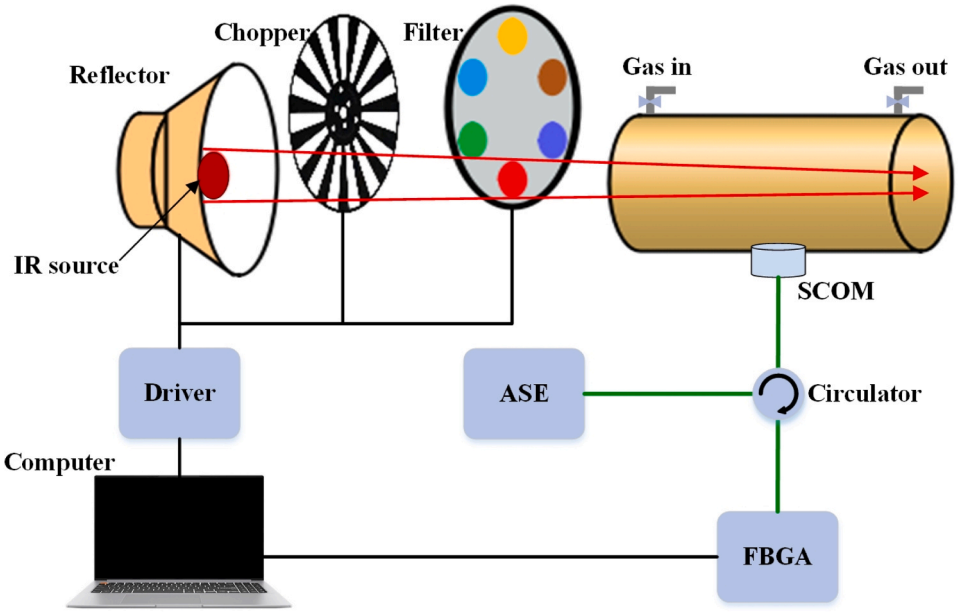

Fig. 4. The structure of the all-optical multi-component gas detection system. (FBGA: Fiber Bragg Grating Analyzer, ASE: Amplified Spontaneous Emission Light Source, SCOM: Silicon Cantilever Optical Microphone, IR Source: Infrared Source).

Table 2
Parameters of the selected passband filters.

Gas	Central wavelength (nm)	Bandwidth (nm)
CO_2	4260	195
CO	4600	190
CH_4	3317	215
C_2H_6	3345	65
C_2H_4	10600	1060
C_2H_2	3050	100

4. Conclusions

In summary, a multicomponent gas sensor based on all-optical non-resonant photoacoustic spectroscopy with silicon cantilever optical microphone is proposed and demonstrated. A FPI-based low-frequency SCOM based on the MEMS technology is designed and fabricated. Experiments show that the fabricated SCOM has high response and low noise level at low-frequency region. The pressure responsivity is measured to be over 96.25 rad/Pa with sensitivity fluctuation less than $\pm$ 1.56 dB between 5 Hz and 250 Hz. And the minimal detectable pressure (MDP) of the sensor is 0.55 μPa·Hz$^{1/2}$ at 200 Hz. The noise performance of the SCOM is far superior to that of commercial condenser microphones [27,28]. A PAC with the gas consumption of

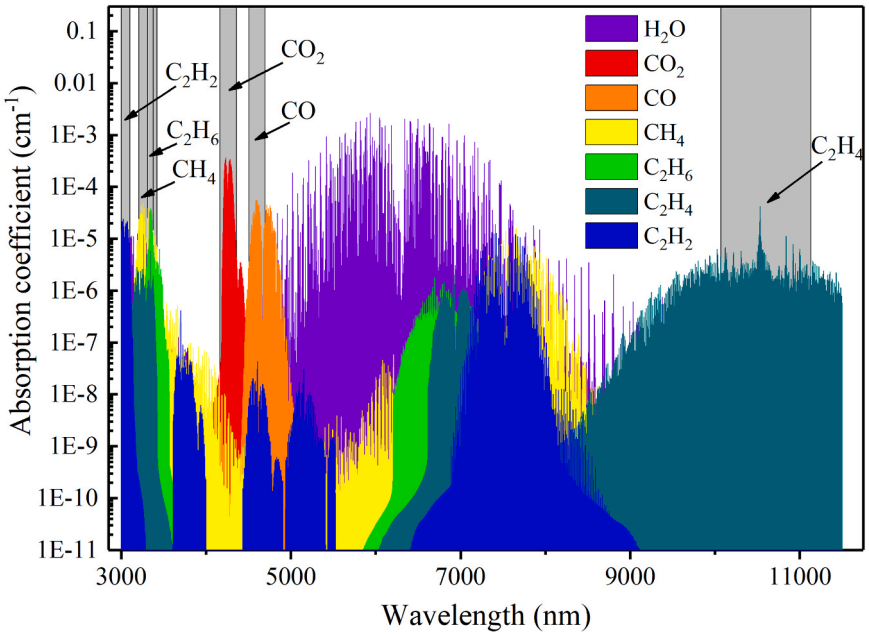

Fig. 5. The absorption coefficients of H_2O and the detected gases: the passband of the selected filters is marked with gray background.

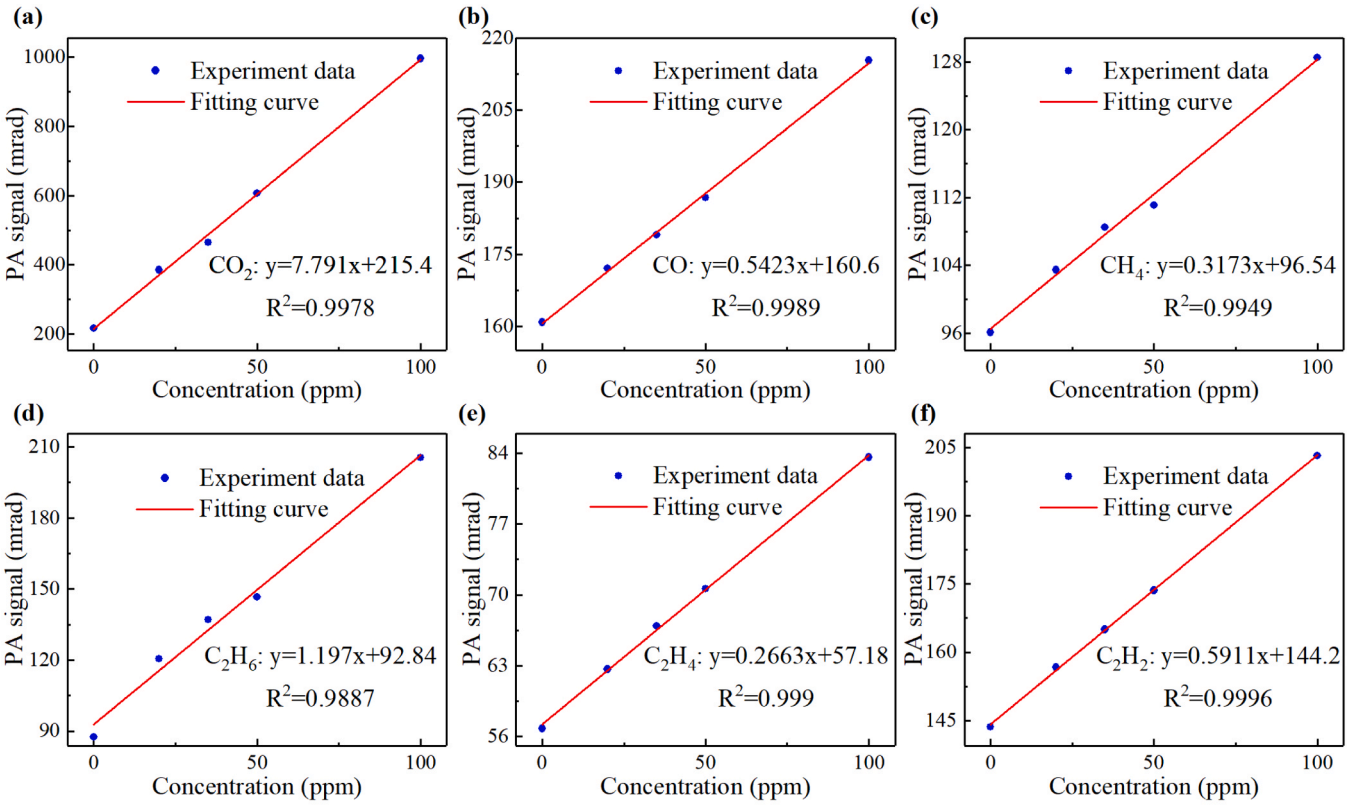

Fig. 6. PA signals of (a) CO_2, (b) CO, (c) CH_4, (d) C_2H_6, (e) C_2H_4 and (f) C_2H_2 with different concentrations.

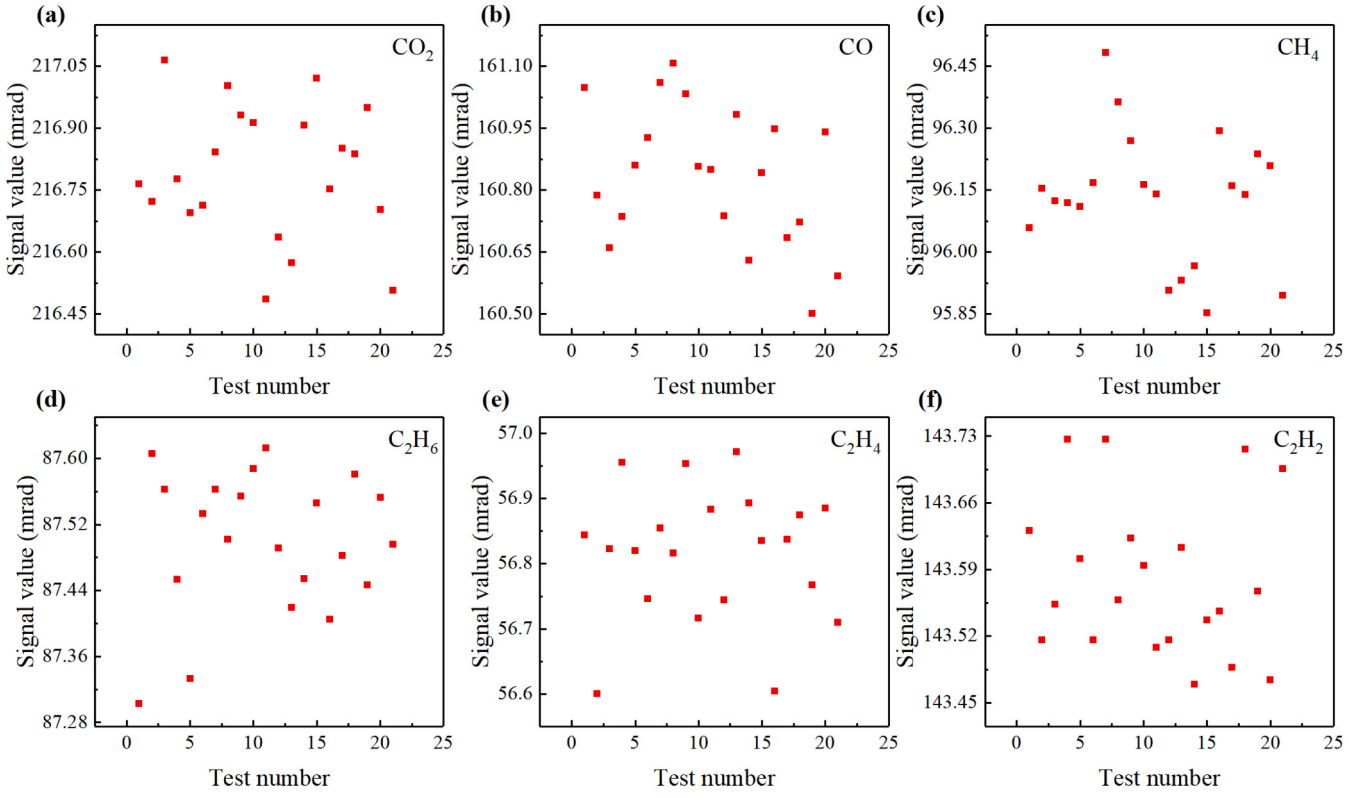

Fig. 7. The background noises with 21 consecutive test data for (a) CO_2, (b) CO, (c) CH_4, (d) C_2H_6, (e) C_2H_4 and (f) C_2H_2.

Table 3
Experimental results for six different gases.

Gas	Noise level	Slope of response (k)	Detection limit (3σ)	R-square value (R^2)
CO_2	0.163 mrad	7.791 mrad/ppm	62.66 ppb	0.9978
CO	0.168 mrad	0.5423 mrad/ppm	929.11 ppb	0.9989
CH_4	0.158 mrad	0.2173 mrad/ppm	1494.97 ppb	0.9949
C_2H_6	0.085 mrad	1.137 mrad/ppm	212.94 ppb	0.9887
C_2H_4	0.102 mrad	0.2663 mrad/ppm	1153.36 ppb	0.999
C_2H_2	0.0823 mrad	0.5911 mrad/ppm	417.61 ppb	0.9996

Table 4
Performance indicators of carbon dioxide sensors based on absorption spectroscopy.

Technology	Operating frequency	Wavelength region	Detection limit	Ref.
QEPAS	28 kHz	Mid-infrared	2.4 ppm	[34]
QEPAS	12.45 kHz	Far-infrared	800 ppb	[35]
Resonant PAS	6215 Hz	Near-infrared	83 ppm	[36]
Resonant PAS	342 Hz	Mid-infrared	223 ppb	[37]
Non-resonant PAS	20 Hz	Mid-infrared	94 ppb	[38]
Non-resonant PAS	10 Hz	Mid-infrared	62.66 ppb	[This paper]

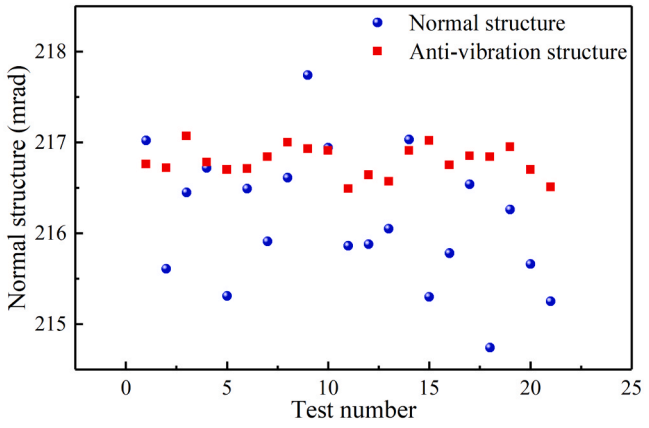

Fig. 8. Noise performance of the all optical PAS system based on normal structure and aseismic structure.

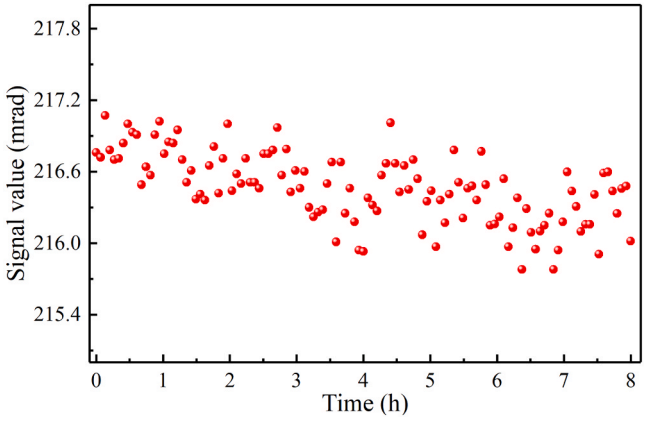

Fig. 9. The tested signals of N_2 for 8 h.

only 2.15 mL based on an aseismic structure is designed and demonstrated. The detection limits (3σ) of CO_2, CO, CH_4, C_2H_6, C_2H_4 and C_2H_2 are calculated to be 62.66 ppb, 929.11 ppb, 1494.97 ppb, 212.94 ppb, 1153.36 ppb and 417.61 ppb, respectively. To the best of our knowledge, the detection limits are optimum among previously reported optical PAS carbon dioxide sensors so far. Comparative experiment based on two structures are conducted to verify the practical performance of the all-optical PAS system by using aseismic structure. The experimental results show that the designed structure has a more stable testing effect, which indicate that the signal jitter of the PAS system with the aseismic structure is reduced by 4.5 times compared with the normal structure. The proposed non-resonant all-optical PAS multi-component gas detection system exhibits the advantages of anti-vibration performance and long term stability, which provides a solution for working in complex environments.

Declaration of Competing Interest

The authors declare that they have no known competing financial interests or personal relationships that could have appeared to influence the work reported in this paper.

Data Availability

No data was used for the research described in the article.

Acknowledgement

This work was supported by NSFC (No. 62275096, No. 62375094); Science Fund for Creative Research Groups of the Nature Science Foundation of Hubei (No. 2021CFA033); NSFC-RS Exchange Programme (No. 62111530153); the Royal Society International Exchanges 2020 Cost Share (NSFC) of United Kingdom (No. IEC\NSFC\201015); Interdiciplinary Research Program (HUST:2023JCYJ046).

References

[1] C. Wang, P. Sahay, Breath analysis using laser spectroscopic techniques: breath biomarkers, spectral fingerprints, and detection limits, Sens-BASEL 9 (2009) 8230–8262, https://doi.org/10.3390/s91008230.
[2] J. Hodgkinson, R.P. Tatam, Optical gas sensing: a review, Meas. Sci. Technol. 24 (2013) 12004, https://doi.org/10.1088/0957-0233/24/1/012004.
[3] N.A. Bakar, A. Abu-Siada, S. Islam, A review of dissolved gas analysis measurement and interpretation techniques, IEEE Electr. Insul M 30 (2014) 39–49, https://doi.org/10.1109/MEI.2014.6804740.
[4] Z. Wei, L. Xu, S. Peng, Q. Zhou, Application of WO3 hierarchical structures for the detection of dissolved gases in transformer oil: a mini review, Front. Chem. 8 (2020), https://doi.org/10.3389/fchem.2020.00188.
[5] S. Lin, J. Chang, J. Sun, P. Xu, Improvement of the detection sensitivity for tunable diode laser absorption spectroscopy: a review, Front. Phys. 10 (2022), https://doi.org/10.3389/fphy.2022.853966.
[6] T. Yang, X. Wu, G. Guo, X. Guo, T. Gong, Y. Tian, X. Sun, X. Qiu, H. Yang, C. Fittshen, C. Li, A miniaturized multipass cell for measurement of O2 concentration in vials based on TDLAS, Opt. Laser Eng. 163 (2023), 107454, https://doi.org/10.1016/j.optlaseng.2022.107454.
[7] Y. Yin, D. Ren, C. Li, R. Chen, J. Shi, Cantilever-enhanced photoacoustic spectroscopy for gas sensing: A comparison of different displacement detection methods, Photoacoustics 28 (2022), 100423, https://doi.org/10.1016/j.pacs.2022.100423.
[8] L. Fu, P. Lu, C. Sima, J. Zhao, Y. Pan, T. Li, X. Zhang, D. Liu, Small-volume highly-sensitive all-optical gas sensor using non-resonant photoacoustic spectroscopy with dual silicon cantilever optical microphones, Photoacoustics 27 (2022), 100382, https://doi.org/10.1016/j.pacs.2022.100382.
[9] C. Zhang, S. Qiao, Y. He, S. Zhou, L. Qi, Y. Ma, Differential quartz-enhanced photoacoustic spectroscopy, Appl. Phys. Lett. 122 (2023), https://doi.org/10.1063/5.0157161.
[10] T. Yang, W. Chen, P. Wang, A review of all-optical photoacoustic spectroscopy as a gas sensing method, Appl. Spectrosc. Rev. 56 (2021) 143–170, https://doi.org/10.1080/05704928.2020.1760875.
[11] L. Zhang, L. Liu, X. Zhang, X. Yin, H. Huan, H. Liu, X. Zhao, Y. Ma, X. Shao, T-type cell mediated photoacoustic spectroscopy for simultaneous detection of multi-component gases based on triple resonance modality, Photoacoustics 31 (2023), 100492, https://doi.org/10.1016/j.pacs.2023.100492.
[12] Z. Gong, G. Wu, X. Jiang, H. Li, T. Gao, M. Guo, F. Ma, K. Chen, L. Mei, W. Peng, Q. Yu, All-optical high-sensitivity resonant photoacoustic sensor for remote CH4

gas detection, Opt. Express. 29 (2021) 13600, https://doi.org/10.1364/OE.424387.
[13] H. Luo, C. Wang, H. Lin, Q. Wu, Z. Yang, W. Zhu, Y. Zhong, R. Kan, J. Yu, H. Zheng, Helmholtz-resonator quartz-enhanced photoacoustic spectroscopy, Opt. Lett. 48 (2023) 1678–1681, https://doi.org/10.1364/OL.481457.
[14] J. Wang, M. Chen, Q. Chen, H. Wang, A resonant photoacoustic cell for hydrogen gas detection, Int. J. Hydrog. Energ 47 (2022) 35940–35946, https://doi.org/10.1016/j.ijhydene.2022.08.166.
[15] Y. Ma, Y. Hong, S. Qiao, Z. Lang, X. Liu, H-shaped acoustic micro-resonator-based quartz-enhanced photoacoustic spectroscopy, Opt. Lett. 47 (2022) 601–604, https://doi.org/10.1364/OL.449822.
[16] Q. Ma, L. Li, Z. Gao, S. Tian, J. Yu, X. Du, Y. Qiao, C. Shan, Near-infrared sensitive differential Helmholtz-based hydrogen sulfide photoacoustic sensors, Opt. Express. 31 (2023) 14851, https://doi.org/10.1364/OE.488835.
[17] Y. Huang, T. Zhang, G. Wang, Y. Xing, S. He, Wavelength-modulated photoacoustic spectroscopy sensor for multi-gas measurement of acetone, methane, and water vapor based on a differential acoustic resonator, Appl. Phys. Lett. 122 (2023), 111105, https://doi.org/10.1063/5.0137679.
[18] Y. Pan, L. Dong, X. Yin, H. Wu, Compact and Highly Sensitive NO2 Photoacoustic Sensor for Environmental Monitoring, Molecules 25 (2020) 1201, https://doi.org/10.3390/molecules25051201.
[19] Y. Ma, R. Lewicki, M. Razeghi, F.K. Tittel, QEPAS based ppb-level detection of CO and N2O using a high power CW DFB-QCL, Opt. Express. 21 (2013) 1008–1019, https://doi.org/10.1364/OE.21.001008.
[20] R. Zhuang, L. Lin, C. Wang, H. Lin, H. Luo, H. Lv, W. Zhu, Y. Zhong, B. Liu, R. Kan, J. Yu, H. Zheng, Quartz-Enhanced Photoacoustic Spectroscopy-Conductance Spectroscopy for Gas Mixture Analysis, Anal. Chem. (2023), https://doi.org/10.1021/acs.analchem.3c01081.
[21] H. Lin, Y. Liu, L. Lin, W. Zhu, X. Zhou, Y. Zhong, M. Giglio, A. Sampaolo, P. Patimisco, F.K. Tittel, J. Yu, V. Spagnolo, H. Zheng, Application of standard and custom quartz tuning forks for quartz-enhanced photoacoustic spectroscopy gas sensing, Appl. Spectrosc. Rev., Ahead–Print. (2022) 1–23, https://doi.org/10.1080/05704928.2022.2070917.
[22] H. Wu, L. Dong, H. Zheng, Y. Yu, W. Ma, L. Zhang, W. Yin, L. Xiao, S. Jia, F. K. Tittel, Beat frequency quartz-enhanced photoacoustic spectroscopy for fast and calibration-free continuous trace-gas monitoring, Nat. Commun. 8 (2017), https://doi.org/10.1038/ncomms15331.
[23] A. Fathy, Y.M. Sabry, I.W. Hunter, D. Khalil, T. Bourouina, Direct absorption and photoacoustic spectroscopy for gas sensing and analysis: a critical review, Laser Photon. Rev. 16 (2022), 2100556, https://doi.org/10.1002/lpor.202100556.
[24] G. Zhang, Z. Xiong, M. Guo, K. Chen, X. Zhao, L. Xu, N. Wang, R. Ni, Z. Gong, W. Peng, Low-Frequency Optical Fiber Fabry-Perot Acoustic Sensor Based on All-Phase Cross-Correlation Demodulation, J. LIGHTWAVE TECHNOL 40 (2022) 7431–7438, https://doi.org/10.1109/JLT.2022.3200332.
[25] M. Guo, K. Chen, G. Zhang, C. Li, X. Zhao, Z. Gong, Q. Yu, High-sensitivity fiber-optic low-frequency acoustic detector based on cross-correlation demodulation, J. Lightwave Technol. 40 (2022) 4481–4488, https://doi.org/10.1109/JLT.2022.3164134.
[26] P. Fan, W. Yan, P. Lu, W. Zhang, W. Zhang, X. Fu, J. Zhang, High sensitivity fiber-optic Michelson interferometric low-frequency acoustic sensor based on a gold diaphragm, Opt. Express. 28 (2020) 25238, https://doi.org/10.1364/OE.402099.
[27] B. Kjær, 1/2" Pressure-field Microphone-Type 4193, https://www.bksv.com/-/media/literature/Product-Data/bp2214.ashx.
[28] GRAS, 1/2" CCP Pressure Standard Microphone Set, High Sensitivity, https://www.grasacoustics.com/products/measurement-microphone-sets/constant-current-power-ccp/product/ss_export/pdf2?product_id=515.
[29] V. Koskinen, J. Fonsen, K. Roth, J. Kauppinen, Progress in cantilever enhanced photoacoustic spectroscopy, VIB Spectrosc. 48 (2008) 16–21, https://doi.org/10.1016/j.vibspec.2008.01.013.
[30] K. Chen, Z. Yu, Q. Yu, M. Guo, Z. Zhao, C. Qu, Z. Gong, Y. Yang, Fast demodulated white-light interferometry-based fiber-optic Fabry-Perot cantilever microphone, Opt. Lett. 43 (2018) 3417–3420, https://doi.org/10.1364/OL.43.003417.
[31] K. Chen, Z. Gong, M. Guo, S. Yu, C. Qu, X. Zhou, Q. Yu, Fiber-optic Fabry-Perot interferometer based high sensitive cantilever microphone, Sens. Actuators A: Phys. 279 (2018) 107–112, https://doi.org/10.1016/j.sna.2018.06.010.
[32] X. Fu, P. Lu, W. Ni, H. Liao, D. Liu, J. Zhang, Phase demodulation of interferometric fiber sensor based on fast Fourier analysis, Opt. Express 25 (2017) 21094, https://doi.org/10.1364/OE.25.021094.
[33] L.S. Rothman, I.E. Gordon, Y. Babikov, A. Barbe, D. Chris Benner, P.F. Bernath, M. Birk, L. Bizzocchi, V. Boudon, L.R. Brown, A. Campargue, K. Chance, E. A. Cohen, L.H. Coudert, V.M. Devi, B.J. Drouin, A. Fayt, J.M. Flaud, R.R. Gamache, J.J. Harrison, J.M. Hartmann, C. Hill, J.T. Hodges, D. Jacquemart, A. Jolly, J. Lamouroux, R.J. Le Roy, G. Li, D.A. Long, O.M. Lyulin, C.J. Mackie, S.T. Massie, S. Mikhailenko, H.S.P. Müller, O.V. Naumenko, A.V. Nikitin, J. Orphal, V. Perevalov, A. Perrin, E.R. Polovtseva, C. Richard, M.A.H. Smith, E. Starikova, K. Sung, S. Tashkun, J. Tennyson, G.C. Toon, V.G. Tyuterev, G. Wagner, The HITRAN2012 molecular spectroscopic database, J. Quant. Spectrosc. Radiat. Transf. 130 (2013) 4–50, https://doi.org/10.1016/j.jqsrt.2013.07.002.
[34] H. Lin, H. Zheng, B.A.Z. Montano, H. Wu, M. Giglio, A. Sampaolo, P. Patimisco, W. Zhu, Y. Zhong, L. Dong, R. Kan, J. Yu, V. Spagnolo, Ppb-level gas detection using on-beam quartz-enhanced photoacoustic spectroscopy based on a 28 kHz tuning fork, Photoacoustics 25 (2022), 100321, https://doi.org/10.1016/j.pacs.2021.100321.
[35] R. De Palo, A. Elefante, G. Biagi, F. Paciolla, R. Weih, V. Villada, A. Zifarelli, M. Giglio, A. Sampaolo, V. Spagnolo, P. Patimisco, Quartz-enhanced photoacoustic sensors for detection of eight air pollutants, Adv. Photon. Res. 4 (2023), https://doi.org/10.1002/adpr.202200353.
[36] Q. Huang, Y. Wei, J. Li, Simultaneous detection of multiple gases using multi-resonance photoacoustic spectroscopy, Sens. Actuators B: Chem. 369 (2022), 132234, https://doi.org/10.1016/j.snb.2022.132234.
[37] L. Liu, H. Huan, A. Mandelis, L. Zhang, C. Guo, W. Li, X. Zhang, X. Yin, X. Shao, D. Wang, Design and structural optimization of T-resonators for highly sensitive photoacoustic trace gas detection, Opt. Laser Technol. 148 (2022), 107695, https://doi.org/10.1016/j.optlastec.2021.107695.
[38] K. Chen, S. Liu, B. Zhang, Z. Gong, Y. Chen, M. Zhang, H. Deng, M. Guo, F. Ma, F. Zhu, Q. Yu, Highly sensitive photoacoustic multi-gas analyzer combined with mid-infrared broadband source and near-infrared laser, Opt. Laser Eng. 124 (2020), 105844, https://doi.org/10.1016/j.optlaseng.2019.105844.

Lujun Fu is now pursuing a PhD degree in optical engineering in School of Optical and Electronic Information at Huazhong University of Science and Technology, China. His research interests include optical sensors and photoacoustic spectroscopy.

Ping Lu is a Professor in School of Optical and Electronic Information at Huazhong University of Science and Technology, China, and Next Generation Internet Access National Engineering Laboratory. She got her Ph. D. degree on optical engineering in 2005 from Huazhong University of Science and Technology. Since 2006, she works at the School of Optical and Electronic Information at Huazhong University of Science and Technology, and starting from 2011, as full Professor. Her research mainly focused on fiber sensors, multicomponent trace gas detection, high sensitivity optical fiber acoustic detection technology, high resolution fiber sensor demodulation technology.

Yufeng Pan received his master's degree in atomic and molecular physics from Shanxi University, China, in 2021. Currently he is a Ph.D. student in optical engineering at Huazhong University of Science and Technology. His research interests include optical sensors and laser spectroscopy techniques.

Yi Zhong is a postgraduate student in School of Optical and Electronic Information at Huazhong University of Science and Technology, China. His research focuses mainly on optical sensing structure and demodulation algorithms

Chaotan Sima is an Associate Professor at Huazhong University of Science and Technology, China. He obtained the PhD degree at the Optoelectronics Research Centre in the University of Southampton UK in 2013. He has been awarded the Marie-Curie Fellowship in 2019 and IEEE senior member since 2021. His research interests include advanced optical gas sensing, planar waveguide devices and holey optical fiber. He has been granted over 10 projects from National Natural Science Foundation of China and the National Key Research and Development Program of China etc. He serves as an editorial member of Optical and Quantum Electronics.

Qiang WU received the B.S. and Ph.D. degrees from Beijing Normal University and Beijing University of Posts and Telecommunications, Beijing, China, in 1996 and 2004, respectively. From 2004–2006, he worked as a Senior Research Associate in City University of Hong Kong. From 2006–2008, he took up a research associate post in Heriot-Watt University, Edinburgh, U.K. From 2008–2014, he worked as a Stokes Lecturer at Photonics Research Centre, Dublin Institute of Technology, Ireland. He is an Associate Professor / Reader with Faculty of Engineering and Environment, Northumbria University, Newcastle Upon Tyne, United Kingdom. His research interests include optical fiber interferometers for novel fiber optical couplers and sensors, nanofiber, microsphere sensors for bio-chemical sensing, the design and fabrication of fiber Bragg grating devices and their applications for sensing, nonlinear fibre optics, surface plasmon resonant and surface acoustic wave sensors. He has over 290 publications in the area of photonics and holds 10 invention patents. He is an Editorial Board Member of Scientific Reports, an Associate Editor of IEEE Sensors Journal and the Journal of Nonlinear Optical Physics & Materials, and an Academic Editor for Journal of Sensors.

Jiangshan Zhang is an Associate Professor in School of Electronic Information and Communications at Huazhong University of Science and Technology, China. He obtained the Ph. D. degree on information and communication Engineering in 2005 from Huazhong University of Science and Technology. His research interests include signal processing and digital communication.

Lingzhi Cui is Assistant Researcher at State Key Laboratory of NBC Protection for Civilian. She received the PhD degree at the College of Chemistry and Molecular Engineering in Peking University in 2020. Her recent research interests include optical sensing materials and optical communication devices.

Deming Liu was born in Hubei Province, China, in January 1957. He received the Graduate degree from Chengdu Institute of Telecommunication (now University of Electronic Science and Technology of China), Chengdu, China, in 1984. Currently, he is the Professor of Huazhong University of Science and Technology, Wuhan, China. His recent research interests include optical access network, optical communication devices, and fiber-optic sensors.